What is the lowest possible reheating temperature?

Steen Hannestad*
Department of Physics, University of Southern Denmark, Campusvej 55, DK-5230 Odense M, Denmark
and NORDITA, Blegdamsvej 17, DK-2100 Copenhagen, Denmark
(Received 12 March 2004; published 9 August 2004)

We study models in which the universe exits reheating at temperatures in the MeV regime. By combining light element abundance measurements with cosmic microwave background and large scale structure data we find a fairly robust lower limit on the reheating temperature of $T_{\rm RH}\gtrsim 4$ MeV at 95% C.L. However, if the heavy particle whose decay reheats the universe has a direct decay mode to neutrinos, there are some small islands left in parameter space where a reheating temperature as low as 1 MeV is allowed. The derived lower bound on the reheating temperature also leads to very stringent bounds on models with n large extra dimensions. For $n=2$ the bound on the compactification scale is $M\gtrsim 2000$ TeV, and for $n=3$ it is 100 TeV. These are currently the strongest available bounds on such models.

DOI: 10.1103/PhysRevD.70.043506 PACS number(s): 98.80.Cq, 98.70.Vc, 98.80.Ft

I. INTRODUCTION

The standard big bang model has been tested thoroughly up to temperatures around 1 MeV where big bang nucleosynthesis occurred. At much higher temperatures the universe is assumed to have undergone inflation, during which the primordial density perturbations are produced.

Towards the end of inflation the inflaton potential steepens so that slow roll is violated, and the universe enters the reheating phase. During this phase all particles which are kinematically allowed are produced, either by direct decay or from the thermal bath produced by the inflaton decay.

Finally the universe enters the radiation dominated phase at a temperature $T_{\rm RH}$, which is a function of the inflaton decay rate. The only certain bound on this reheating temperature comes from big bang nucleosynthesis, and has in several previous studies been found to be around 1 MeV [1–4].

It should be noted that even if the reheating temperature after inflation is much higher there can still be subsequent ''reheating'' phases, in the sense that reheating is defined to be a period where the energy density is dominated by an unstable nonrelativistic particle species. In standard reheating this is the inflaton, but in supersymmetric models it could for instance be the gravitino.

In the present paper we update previous calculations of this reheating phenomenon, using data from cosmic microwave background and large scale structure observations. Furthermore we extend the analysis to include the possibility of having a direct decay mode of the heavy particle into light neutrinos. If the heavy particle is a scalar this decay is normally suppressed by a factor $(m_\nu/m_\phi)^2$ because of the necessary helicity flip. However, the heavy particle could either be a nonscalar particle, or it could be a pseudoscalar like the majoron which couples only to neutrinos. Even though such models are slightly contrived it is of interest to study whether the temperature bound on reheating is significantly affected by the possibility of direct decay into neutrinos.

In Sec. II we discuss the set of Boltzmann equations necessary to follow the evolution of all particle species. In Sec. III present results of the numerical solution of these equation, and in Sec. IV we compare model predictions with observational data. Finally, Sec. V is a review of other astrophysical constraints on heavy, decaying particles, and Sec. VI contains a discussion.

II. BOLTZMANN EQUATIONS

We follow the evolution of all particles by solving the Boltzmann equation for each species,

$$\frac{\partial f}{\partial t}-Hp\frac{\partial f}{\partial p}=C_{\rm coll}, \tag{1}$$

where $C_{\rm coll}$ is the collision operator describing elastic and inelastic collisions.

A. Neutrinos

Neutrinos interact with the electromagnetic plasma via weak interactions. A comprehensive treatment of this can for instance be found in Ref. [5]. The collision integrals can be written as [5]

$$C_{{\rm coll},i}(f_1)=\frac{1}{2E_1}\int\frac{d^3\mathbf{p}_2}{2E_2(2\pi)^3}\frac{d^3\mathbf{p}_3}{2E_3(2\pi)^3}\frac{d^3\mathbf{p}_4}{2E_4(2\pi)^3}\times(2\pi)^4\delta^4(p_1+p_2-p_3+p_4)\times\Lambda(f_1,f_2,f_3,f_4)S|M|_{12\to 34,i}, \tag{2}$$

where $S|M|_{12\to 34,i}$ is the spin-summed and averaged matrix element including the symmetry factor $S=1/2$ if there are identical particles in initial or final states. The phase-space factor is $\Lambda(f_1,f_2,f_3,f_4)=f_3f_4(1-f_1)(1-f_2)-f_1f_2(1-f_3)(1-f_4)$.

This collision integral can be reduced to 2 dimensions using the method developed in Ref. [5]. However, if Pauli blocking and interactions involving only neutrinos are neglected the integrals can in fact be reduced to 1 dimension, as described in Ref. [2]. In the following we use this method.

*Electronic address: hannestad@fysik.sdu.dk

 ©2004 The American Physical Society

The quantitative error resulting from this is quite small (it is at most a few percent, as stated in Ref. [2]).

In addition to standard weak interactions we allow for a direct decay of ϕ to neutrinos, $\phi \to \nu\bar{\nu}$. If ϕ is nonrelativistic then each neutrino is born with momentum $m_\phi/2$ and in this case the collision integral is

$$C_{\phi\to\nu_i\bar{\nu}_i} = b_{\nu_i}\frac{2\pi^2}{(m_\phi/2)^2}\Gamma_\phi n_\phi \delta(p_\nu - m_\phi/2), \tag{3}$$

where b_{ν_i} is the branching ratio into neutrino species i, and Γ_ϕ is the decay rate of the heavy particle. For simplicity we assume equal branching ratios into all neutrino species. Even if this is not the case the neutrino distribution functions will be almost equilibrated by oscillations [6]. This means that $b_{\nu_e} \simeq b_{\nu_\mu} \simeq b_{\nu_\tau} \simeq b_\nu/3$. An interesting possibility, which we do not consider here, is the presence of sterile neutrinos. For instance, if the LSND result is confirmed then four neutrino mass eigenstates are needed, one of which must be sterile. In standard cosmology this possibility is severely constrained, but in models with extremely low reheating temperature the bound can be relaxed [7].

Note that if one assumes that neutrinos are in kinetic equilibrium so that they can be described by a single temperature T_ν it is in fact possible to solve the Boltzmann equation semianalytically [8]. However, this is a very poor approximation for the case when there is a direct decay mode $\phi \to \nu\bar{\nu}$.

B. ϕ

We assume the heavy particle to be completely nonrelativistic. If that is the case then the Boltzmann equation can be integrated to give the following equation for the evolution of the energy density:

$$\dot{\rho}_\phi = -\Gamma_\phi \rho_\phi - 3H\rho_\phi, \tag{4}$$

i.e. there are no inverse decays. This is a good approximation for all the cases covered in the present work.

We only work with masses which are low enough that there are no hadronic decay channels open. This of course severely restricts the possible models. However, if there is a hadronic branching ratio then the minimum allowed reheating temperature increases dramatically [2], and we are investigating what the *lowest* possible reheating temperature is.

C. Electromagnetic plasma

The evolution of the photon temperature can then be found from the equation of energy conservation

$$\frac{d\rho_T}{dt} = -3H(\rho_T + P_T), \tag{5}$$

where ρ_T and P_T are the total energy density and the total pressure respectively. This equation can be rewritten as an evolution equation for T_γ

$$\frac{dT_\gamma}{dt} = -\frac{-(1-b_\nu)\rho_\phi\Gamma_\phi + 4H\rho_\gamma + 3H(\rho_e + P_e) + 4H\rho_\nu + d\rho_\nu/dt}{\partial\rho_\gamma/\partial T_\gamma + \partial\rho_e/\partial T_\gamma}. \tag{6}$$

D. Scale factor

Finally we solve the Friedmann equation to find the scale factor as a function of time

$$H = \frac{\dot{a}}{a} = \sqrt{\frac{8\pi G\rho_T}{3}}. \tag{7}$$

Altogether we solve Eq. (7) together with Eq. (1) for each neutrino species, Eq. (4) for ϕ, and Eq. (6) for the photon temperature, to obtain $a(t)$, $T_\gamma(t)$, $\rho_\phi(t)$, and $f_{\nu_i}(t)$.

E. Initial conditions

Following convention we define the reheating temperature of the universe to be when

$$\Gamma_\phi = 3H(T_{\rm RH}). \tag{8}$$

To a reasonable approximation the universe is radiation dominated at this point so that

$$H = \left(\frac{g_*\pi^2}{90}\right)^{1/2}\frac{T_{\rm RH}^2}{M_{\rm Pl}}, \tag{9}$$

where $M_{\rm Pl} = 2.4\times10^{18}$ GeV is the reduced Planck mass and g_* is the number of degrees of freedom.

This means that there is a one to one correspondence between Γ_ϕ and $T_{\rm RH}$,

$$T_{\rm RH,MeV} \simeq 0.7\Gamma_{\rm s^{-1}}^{1/2}, \tag{10}$$

where $g_* = 10.75$ has been used. Note that the constant of proportionality is somewhat arbitrary (although it should always be of order 1), and just gives a rough idea about the thermal temperature when the universe enters the standard radiation dominated phase. Another reasonable definition would have been $\Gamma_\phi = H(T_{\rm RH})$ which would lead to the relation $T_{\rm RH,MeV} \simeq 0.4\Gamma_{\rm s^{-1}}^{1/2}$. The bottom line is that $T_{\rm RH}$ is just an effective parameter, the exact definition of which is somewhat arbitrary.

As long as the initial time is set so that $t_i \ll t(T_{\rm RH})$ *and* $T_{\rm max} \gtrsim T_{{\rm D},\nu}$, where $T_{\rm max}$ is the maximum temperature

reached by the plasma after time t_i and $T_{\mathrm{D},\nu}$ is the neutrino decoupling temperature then the final outcome is independent of initial conditions. The universe starts out being strongly matter dominated and the final neutrino energy density, as well as the light element abundances depend only on Γ_ϕ, m_ϕ, and b_ν. The initial time is found from the Friedmann equation by assuming complete domination of ϕ so that $t_i = \frac{2}{3}[8\pi G\rho_{\phi,i}/3]^{-1/2}$.

F. Nucleosynthesis

One of the main observables from the epoch around neutrino decoupling is the abundance of light elements, mainly helium and deuterium. In order to calculate these abundances we have modified the Kawano nucleosynthesis code [9]. First it has been modified to incorporate the modified temperature evolution, and second the subroutines used to calculate weak interaction rates for $n \leftrightarrow p$ have been modified to incorporate the full numerical electron neutrino distribution coming from the solution of the coupled Boltzmann equations. This allows us to calculate the abundance of ^{4}He and D for the various models.

Although the Kawano code is less precise than some newer Big Bang Nucleosynthesis (BBN) codes (see for instance Refs. [10,11]) it is more than sufficiently accurate for our purposes. The reason is that incomplete neutrino decoupling only enters via a modified expansion rate and the weak *n-p* conversion rates, both of which are treated accurately by the Kawano code.

III. NUMERICAL RESULTS

We have solved the set of coupled Boltzmann equations for all species for the free parameters, m_ϕ, Γ_ϕ, and b_ν.

The main output from this is the relativistic energy density in neutrinos, parametrized in units of the energy density of a standard model neutrino, ρ_{ν_0},

$$N_\nu = \frac{\rho_{\nu_e} + \rho_{\nu_\mu} + \rho_{\nu_\tau}}{\rho_{\nu_0}}. \tag{11}$$

A. $b_\nu = 0$

If $b_\nu = 0$ then the equations become independent of m_ϕ and this case has already been covered in Ref. [2]. We present this as our first case in order to compare results with those of Ref. [2]. Figure 1 shows the effective number of neutrino species, N_ν, after complete decay of ϕ. This figure is identical to Fig. 4 in Ref. [2].

We also test whether our results are independent of initial conditions. In Fig. 2 we show $T_\gamma(t)$ and $\rho_\phi(t)$ for $\Gamma_\phi = 6.4\ \mathrm{s}^{-1}$ for two different initial times, $t_i = 1.8\times10^{-3}$ s and $t_i = 8.8\times10^{-3}$ s. In both cases we assume an initial photon temperature of 2.3 MeV (we could equally well have chosen an initial temperature of 0). While the maximum temperature reached is clearly dependent on t_i, T_γ and ρ_ϕ quickly become indistinguishable, and as long as the temperature where this happens is greater than the neutrino decoupling temperature all final results are independent of t_i. Furthermore, as expected [2], the photon temperature scales as $T_\gamma \propto t^{-1/4}$ during the matter dominated period and shifts to the usual $T_\gamma \propto t^{-1/2}$ once the universe becomes radiation dominated (except for a small deviation due to heating by e^+e^- annihilation).

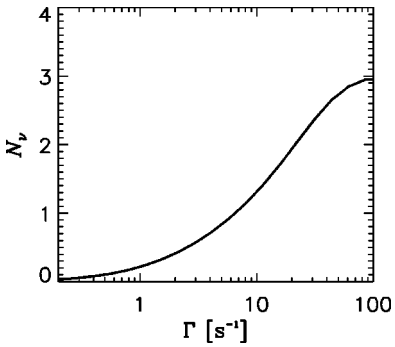

FIG. 1. The effective number of neutrino species as a function of Γ_ϕ when there is no direct decay into neutrinos, $b_\nu = 0$.

B. $b_\nu \neq 0$

Next we cover the case when $b_\nu \neq 0$. This is much more complicated to solve numerically because of the presence of the delta function $\delta(p_\nu - m_\phi/2)$ and the fact that the solution now depends on both b_ν and m_ϕ. In Fig. 3 we show N_ν for different values of Γ_ϕ and b_ν. From this figure is clear that when b_ν is small the effective number of neutrino species becomes independent of m_ϕ and increasing with Γ_ϕ, with $N_\nu \to 3$ for $\Gamma_\phi \to \infty$.

For the opposite case when $b_\nu = 1$ (only decay to neutrinos) the situation is the opposite. When $\Gamma \to \infty$ the limiting value is again $N_\nu = 3$. This corresponds to the case when ϕ decays into neutrinos, but the effective neutrino temperature after complete ϕ decay is higher than T_D.

When $\Gamma \to 0$ the effective number of neutrino species goes to infinity. This corresponds to the case when ϕ decays so

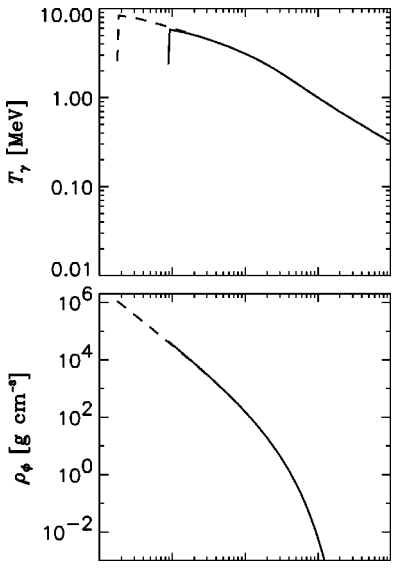

FIG. 2. T_γ and ρ_ϕ as functions of time for $\Gamma_\phi = 6.4\ \mathrm{s}^{-1}$, $b_\nu = 0$ and two different initial times. The full line is for $t_i = 8.8\times10^{-3}$ s, whereas the dashed is for $t_i = 1.8\times10^{-3}$ s.

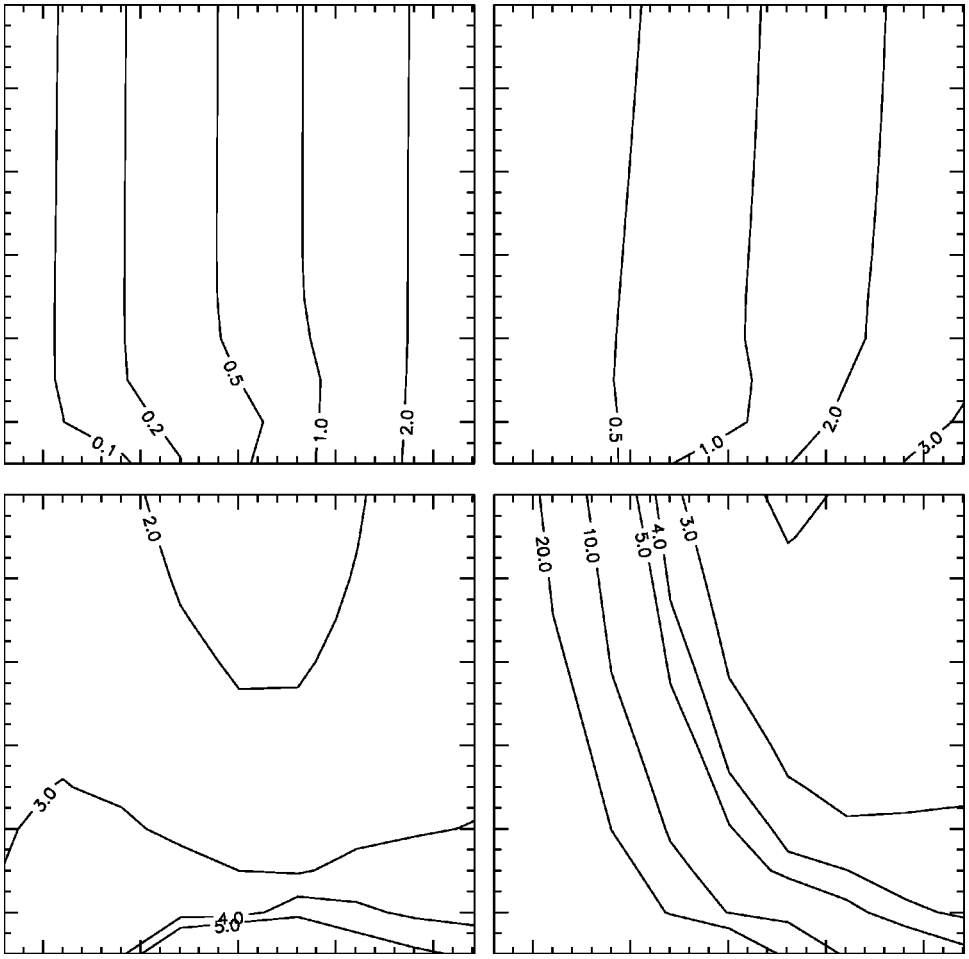

FIG. 3. Contour plot of N_ν for different m_ϕ and Γ_ϕ. The top left plot is for $b_\nu=0.1$, the top right for $b_\nu=0.5$, the bottom left for $b_\nu=0.9$, and the bottom right for $b_\nu=1.0$.

slowly that the produced neutrinos never equilibrate with the electromagnetic plasma, leaving only neutrinos.

However, there is a large intermediate region where $N_\nu<3$, even for $b_\nu=1$. The reason for this unexpected feature can be explained as follows: When high energy neutrinos ($E\gg T$) are produced by direct ϕ decay they have a very high annihilation cross section to e^+e^-, because the cross section goes as E^2. However, the produced electrons and positrons are immediately converted into a sea of low energy e^+, e^-, and γ because of electromagnetic interactions. This means that the production rate of neutrinos is much lower. In the case where the reheating temperature is very high this does not matter because the universe still has time to thermalize completely after ϕ decay. However, if $T_{\rm RH}\sim T_{\rm D}$, this is not possible and the result is that $N_\nu<3$ because of the very efficient conversion of neutrinos into e^+e^-. Notice also that this effect becomes less pronounced when m_ϕ decreases because neutrinos are born with energies closer to $3T$, and the mismatch between forward and backward rates becomes smaller.

In Figs. 4 and 5 this effect can be seen directly on the distribution functions. In Fig. 4, which shows $b_\nu=1$, $\Gamma_\phi=6.4\ {\rm s}^{-1}$, and $m_\phi=120$ MeV, it can be seen that the distribution function is higher than thermal at high energies because of ϕ decay. However, there are fewer low energy neutrinos because of the inefficient production via e^+e^- annihilation.

Conversely, in Fig. 5, which shows $b_\nu=1$, $\Gamma_\phi=50\ {\rm s}^{-1}$, and $m_\phi=120$ MeV, it can be seen that the decay rate is high enough that neutrinos equilibrate with the electromagnetic plasma, except for a small deviation around $p_\nu=m_\phi/2$. This subsequently leads to $N_\nu\simeq3$ after complete ϕ decay.

IV. COMPARISON WITH DATA

In order to constrain the parameters b_ν, Γ_ϕ, and m_ϕ we compare the predicted values of N_ν, ^{4}He, and D with the

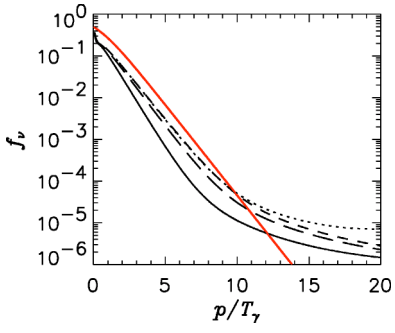

FIG. 4. The distribution function for ν_e for different values of T_γ when $\Gamma=6.4\ {\rm s}^{-1}$, $b_\nu=1$, and $m_\phi=120$ MeV. The dotted line is for $T_\gamma=2.18$ MeV, the dashed for $T_\gamma=0.42$ MeV, the long-dashed for $T_\gamma=0.19$ MeV, and the full line for $T_\gamma=0.01$ MeV. The full gray (red) line is an equilibrium distribution with $T_\nu=T_\gamma$.

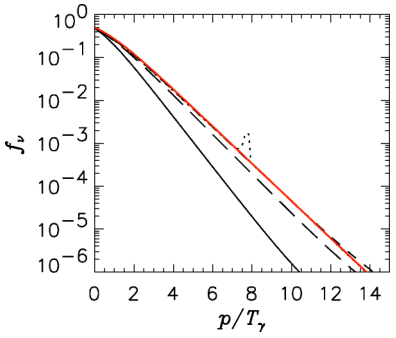

FIG. 5. The distribution function for ν_e for different values of T_γ when $\Gamma=50\ \mathrm{s}^{-1}$, $b_\nu=1$, and $m_\phi=120$ MeV. The dotted line is for $T_\gamma=7.7$ MeV, the dashed for $T_\gamma=0.93$ MeV, the long-dashed for $T_\gamma=0.23$ MeV, and the full line for $T_\gamma=0.01$ MeV. The full gray (red) line is an equilibrium distribution with $T_\nu=T_\gamma$.

observationally determined values. In addition to the parameters directly related to ϕ the nucleosynthesis outcome depends crucially on the baryon density, $\eta=n_B/n_\gamma$.

Taken at face value the recent cosmic microwave background (CMB) data from the WMAP satellite constrain η tightly. However, it has been shown that there is a significant correlation between η and N_ν in the CMB data. This means that it is not possible to take CMB constraint on η directly and apply it to the nucleosynthesis calculations. Rather a full CMB likelihood analysis for N_ν and η must be carried out. This can then be combined with the nucleosynthesis likelihood analysis for b_ν, Γ_ϕ, m_ϕ, and η.

First the following subsection covers the current observational status, then the next covers the constraints on decay parameters which can be obtained.

A. Observational data

1. Light element abundances

The primordial helium abundance has been derived by two independent groups. Fields and Olive [12] find the value

$$Y_P=0.238\pm0.002\pm0.005, \tag{12}$$

whereas Izotov and Thuan [13] find

$$Y_P=0.244\pm0.002\pm0.005. \tag{13}$$

Because of this inconsistency we blow up the error bars on Y_P and use the value

$$Y_P=0.238\pm0.015, \tag{14}$$

which encompasses the allowed regions of both observational determinations.

The most recent determination of the primordial deuterium abundance has yielded the value [14]

$$\mathrm{D/H}=(2.78\pm0.29)\times10^{-5}. \tag{15}$$

A determination of the primordial lithium abundance has also been performed by several groups. However, this measurement is prone to large systematics and we refrain from using it here.

2. Cosmic microwave background

The CMB temperature fluctuations are conveniently described in terms of the spherical harmonics power spectrum

$$C_l\equiv\langle|a_{lm}|^2\rangle, \tag{16}$$

where

$$\frac{\Delta T}{T}(\theta,\phi)=\sum_{lm} a_{lm}Y_{lm}(\theta,\phi). \tag{17}$$

Since Thomson scattering polarizes light there are additional power spectra coming from the polarization anisotropies. The polarization can be divided into a curl-free (E) and a curl (B) component, yielding four independent power spectra: $C_{T,l}$, $C_{E,l}$, $C_{B,l}$ and the temperature E-polarization cross correlation $C_{TE,l}$.

The WMAP experiment has reported data on $C_{T,l}$ and $C_{TE,l}$, as described in Refs. [15–17].

We have performed the likelihood analysis using the prescription given by the WMAP collaboration which includes the correlation between different C_l's [15–17]. Foreground contamination has already been subtracted from their published data.

3. Large scale structure

The 2dF Galaxy Redshift Survey (2dFGRS) [18] has measured the redshifts of more than 230 000 galaxies with a median redshift of $z_\mathrm{m}\approx0.11$. An initial estimate of the convolved, redshift-space power spectrum of the 2dFGRS has been determined [19] for a sample of 160 000 redshifts. On scales $0.02<k<0.15h\ \mathrm{Mpc}^{-1}$ the data are robust and the shape of the power spectrum is not affected by redshift-space or nonlinear effects, though the amplitude is increased by redshift-space distortions. A potential complication is the fact that the galaxy power spectrum may be biased with respect to the matter power spectrum, i.e. light does not trace mass exactly at all scales. This is often parametrized by introducing a bias factor

$$b^2(k)\equiv\frac{P_\mathrm{g}(k)}{P_\mathrm{m}(k)}, \tag{18}$$

where $P_\mathrm{g}(k)$ is the power spectrum of the galaxies, and $P_\mathrm{m}(k)$ is the matter power spectrum. However, we restrict our analysis of the 2dFGRS power spectrum to scales $k<0.15\ \mathrm{h\ Mpc}^{-1}$ where the power spectrum is well described by linear theory. On these scales, two different analyses have demonstrated that the 2dFGRS power spectrum is consistent with linear, scale-independent bias [20,21]. Thus, the shape of the galaxy power spectrum can be used straightforwardly to constrain the shape of the matter power spectrum.

The only parameters which affect CMB and structure formation are the baryon density, η, and the relativistic energy

density at late times, parametrized by N_ν [24,25] (see also Refs. [26–33]). It is therefore relatively straightforward to perform the CMB+LSS likelihood analysis.

It should also be noted here that there are other cosmological data sets which could have been used for the analysis. The Sloan Digital Sky Survey (SDSS) [22,23] is at present comparable in size to the 2dF survey, although it will eventually be significantly bigger. Some likelihood analyses also include CMB other than WMAP, particularly on smaller scales. With the present data the final outcome of the analysis would change very little by including this additional data. That this is the case can for instance be seen from the fact that the CMB+large scale structure (LSS) data analysis for N_ν is very almost identical in Refs. [34] and [35], even though different data sets are used.

B. Likelihood analysis

Nucleosynthesis is affected both by the expansion rate around $T\sim 0.1-1$ MeV, and by the electron neutrino distribution function. The reason is that electron neutrino enter directly in the weak reactions which interconvert protons and neutrons.

The specific neutrino distributions are therefore found as functions of temperature and used in a modified version of the Kawano BBN code [9]. This is then used to calculate primordial abundances of deuterium and helium.

For calculating the theoretical CMB and matter power spectra we use the publicly available CMBFAST package [36]. As the set of cosmological parameters we choose Ω_m, the matter density, Ω_b, the baryon density, H_0, the Hubble parameter, τ, the optical depth to reionization, Q, the normalization of the CMB power spectrum, b, the bias parameter, and the effective number of neutrino species N_ν, found from the solution of the Boltzmann equations. We assume neutrinos to be almost massless. We restrict the analysis to geometrically flat models $\Omega_m+\Omega_\Lambda=1$.

For each individual model we calculate χ^2 in the following way: Given a theoretical CMB spectrum the χ^2 of the WMAP data is calculated using the method described in Ref. [17]. With regards to the 2dF data we use the data points and window functions from Ref. [37] (http://www.hep.upenn.edu/~max/2df.html). 68% and 95% confidence levels from the data are calculated from $\Delta\chi^2=2.31$ and 6.17 respectively.

1. $b_\nu=0$

In Fig. 6 we show 68% and 95% exclusion limits for η and Γ_ϕ from BBN, CMB, and LSS. The top panel for BBN only is very similar to Fig. 8 in Ref. 2, except that we use slightly different bounds on light element abundances. From BBN alone the 95% bound on $T_{\rm RH}$ is roughly 0.6 MeV. However this bound is achieved for relatively low η, whereas CMB+LSS strongly prefer a high value of η. Therefore combining the BBN and CMB+LSS constraints removes the low $T_{\rm RH}$ region and increases the lower bound to 3.9 MeV.

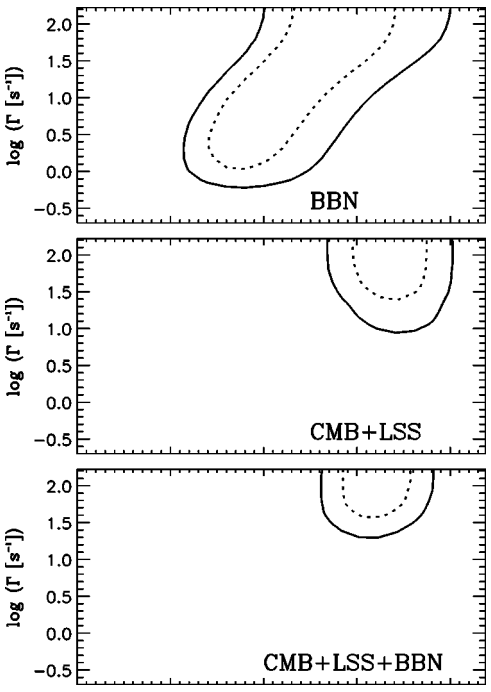

FIG. 6. 68% and 95% confidence exclusion plot of the parameters $\eta_{10}\equiv 10^{10}\times\eta$ and Γ_ϕ for the case when $b_\nu=0$.

2. $b_\nu\neq 0$

Apart from the fact that N_ν depends on b_ν there is a second effect which is just a important. When $b_\nu\neq 0$ there are more high energy neutrinos. Around weak freezeout there are many more protons than neutrons. When $E_\nu \gg m_n-m_p$ the weak absorption cross section is equal on protons and neutrons. This means that additional neutrinos at high energies will have the net effect of converting protons into neutrons, so that in the end more helium is produced. Note that this is the opposite effect of just increasing the weak interaction rates, in which case *less* helium would be produced. The phenomenon is quite similar to what happens if ϕ has a hadronic decay channel. In that case pions and kaons will be produced, which subsequently convert protons to neutrons and lead to overproduction of helium.

In Fig. 7 we show 68%, 95%, and 99.99% confidence exclusion plots for Γ_ϕ and m_ϕ, marginalized over η.

Both when b_ν is small and when $b_\nu=1$ the bound on $T_{\rm RH}$ becomes independent of m_ϕ. In both cases the 95% bound is $T_{\rm RH}\gtrsim 4$ MeV.

However, there is an intermediate regime for b_ν which allows for much lower values of $T_{\rm RH}$. The reason for this can be seen directly from Fig. 3, i.e. there is an intermediate range where N_ν can be kept close to 3, even for low Γ_ϕ. However, for large masses (which is of course by far the most likely) there is no allowed region. The reason is the one given in the previous section: More high energy neutrinos will produce more helium, and this in turn will conflict with observations.

The final outcome is that for almost all values of m_ϕ and b_ν there is a robust lower bound on $T_{\rm RH}$ which is around 4 MeV. However there is a small region where $b_\nu\sim 0.9$, m_ϕ

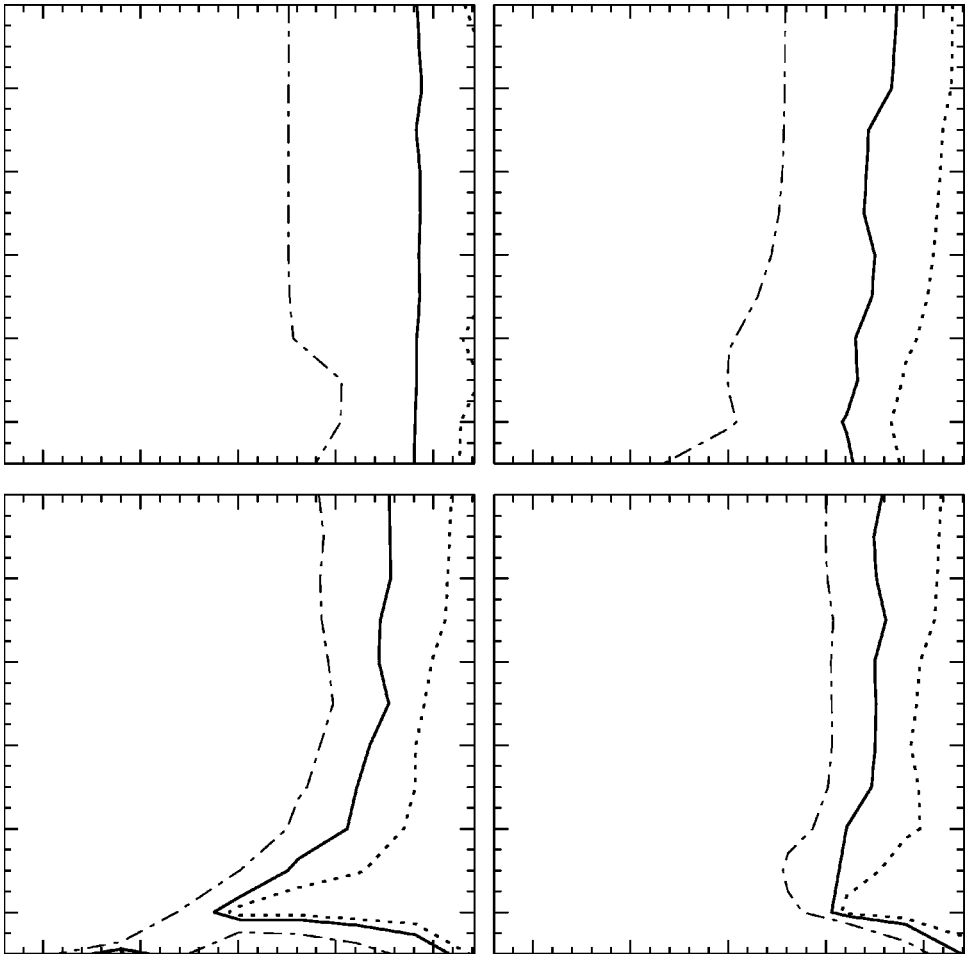

FIG. 7. 68%, 95%, and 99.99% confidence exclusion plot of the parameters Γ_ϕ and m_ϕ using all available data (CMB+LSS +BBN). The top left plot is for $b_\nu=0.1$, the top right for $b_\nu=0.5$, the bottom left for $b_\nu=0.9$, and the bottom right for $b_\nu=1.0$.

$\lesssim$40 MeV where a reheating temperature as low as roughly 1 MeV is allowed.

It should perhaps be noted here that if ϕ is heavy ($m_\phi \gtrsim 2m_\pi$) then there is likely to be some hadronic branching in the decay. If this is the case then the bound is strengthened significantly [38].

V. OTHER CONSTRAINTS

If ϕ is a scalar then the decay rate to neutrinos is normally suppressed by a factor m_ν^2 because of the necessary helicity flip. Therefore the simplest assumption is that ϕ has no branching into neutrinos. If for instance the heavy particle is a pseudoscalar like the axion, then there is an upper bound on the coupling to photons [39,40], $g_{\phi\gamma} \leqslant 0.6 \times 10^{-10}\ \mathrm{GeV}^{-1}$ for $m_\phi \lesssim 30$ keV. For higher masses the bound is significantly weaker. However, even if this bound is used together with the decay width $\Gamma_{\phi\to 2\gamma}=g_{\phi\gamma}^2 m_\phi^3/64\pi$ then we find that

$$\Gamma_{\phi\to 2\gamma} \lesssim 50 m_{\phi,10\ \mathrm{MeV}}^3\ \ \mathrm{s}^{-1}, \tag{19}$$

which is easily satisfies for the parameter space we are considering.

On the other hand, if ϕ is a particle like the majoron which couples only to neutrinos then the decay width is [41]

$$\Gamma_{\phi\to\nu\bar{\nu}}=\frac{g_{\phi\nu}^2 m_\phi}{16\pi} \sim 3\times 10^{19} g_{\phi\nu}^2 m_{\phi,\mathrm{MeV}}\ \ \mathrm{s}^{-1} \tag{20}$$

The bound on the dimensionless coupling constant comes from BBN as well as supernova considerations and is of order 10^{-6}–10^{-5} for majorons in the MeV mass range [40,42]. For more massive majorons the bound weakens. Again it is clear that the decay parameters which we consider here are not excluded by any other astrophysical or experimental data.

The final conclusion is that heavy, decaying particles such as the ones considered here cannot be directly excluded by any current data. Furthermore a branching ratio into neutrinos can be anywhere from 0 to 1.

VI. CONCLUSION

We have carefully calculated constraints on models with extremely low reheating temperature, where a massive particle decays around $T\sim 1$ MeV. By combining constraints on light element abundances with constraints on η and N_ν from CMB and large scale structure we derived a fairly robust limit of

$$T_{\mathrm{RH}} \gtrsim 4\ \ \mathrm{MeV}. \tag{21}$$

This bound is a significant improvement over the previous bound of $T_{\rm RH} \gtrsim 0.7$ MeV, calculated from BBN alone. It is interesting that the lower bound is significantly higher than the $n \leftrightarrow p$ conversion freezeout temperature, $T \sim 0.8$ MeV, and even higher than the neutrino decoupling temperature $T_{\rm D} \sim 2$ MeV. This shows that even small residual effects from a modified neutrino decoupling history can be measured with present observational data.

Models with reheating temperature in the MeV regime are in general difficult to reconcile with such features as baryogenesis (see for instance Ref. [43] for a discussion of this issue). However, in models with large extra dimensions a low reheating temperature is essential in order to avoid overproduction of massive Kaluza-Klein graviton states. This means that we can use our present bound to derive limits on the compactification scale in such models. For the case of two extra dimensions the bound is $M \gtrsim 2000$ TeV and for $n = 3$ it is $M \gtrsim 100$ TeV. This bound is somewhat stronger than the bound coming from considerations of neutron star cooling and gamma ray emission.

Finally, it should be noted that future CMB and large scale structure data will allow for a much more precise determination of both N_ν and $\Omega_b h^2$ (see for instance Refs. [31,44]). This in turn means that in the future the bound on the reheating temperature can be strengthened significantly.

ACKNOWLEDGMENTS

We acknowledge use of the publicly available CMBFAST package written by Uros Seljak and Matias Zaldarriaga [36], as well as the nucleosynthesis code written by Lawrence Kawano [9]. I wish to thank P. Serpico for comments.

[1] M. Kawasaki, K. Kohri, and N. Sugiyama, Phys. Rev. Lett. **82**, 4168 (1999).
[2] M. Kawasaki, K. Kohri, and N. Sugiyama, Phys. Rev. D **62**, 023506 (2000).
[3] G.F. Giudice, E.W. Kolb, and A. Riotto, Phys. Rev. D **64**, 023508 (2001).
[4] G.F. Giudice, E.W. Kolb, A. Riotto, D.V. Semikoz, and I.I. Tkachev, Phys. Rev. D **64**, 043512 (2001).
[5] S. Hannestad and J. Madsen, Phys. Rev. D **52**, 1764 (1995).
[6] A.D. Dolgov, S.H. Hansen, S. Pastor, S.T. Petcov, G.G. Raffelt, and D.V. Semikoz, Nucl. Phys. **B632**, 363 (2002).
[7] G. Gelmini, S. Palomares-Ruiz, and S. Pascoli, astro-ph/0403323.
[8] P. Adhya, D.R. Chaudhuri, and S. Hannestad, Phys. Rev. D **68**, 083519 (2003).
[9] L. Kawano, FERMILAB-PUB-92-04-A
[10] V. Barger, J.P. Kneller, H.S. Lee, D. Marfatia, and G. Steigman, Phys. Lett. B **566**, 8 (2003).
[11] A. Cuoco, F. Iocco, G. Mangano, G. Miele, O. Pisanti, and P.D. Serpico, astro-ph/0307213.
[12] B.D. Fields and K.A. Olive, Astrophys. J. **506**, 699 (1998).
[13] Y.I. Izotov and T.X. Thuan, Astrophys. J. **500**, 188 (1998).
[14] S. Burles and D. Tytler, Astrophys. J. **499**, 699 (1998); J.M. O'Meara *et al.*, *ibid.* **552**, 718 (2001); D. Kirkman *et al.*, Astrophys. J., Suppl. (to be published).
[15] C.L. Bennett *et al.*, Astrophys. J., Suppl. **148**, 1 (2003).
[16] D.N. Spergel *et al.*, Astrophys. J., Suppl. **148**, 175 (2003).
[17] L. Verde *et al.*, Astrophys. J., Suppl. **148**, 195 (2003).
[18] 2dFGRS Team, M. Colless *et al.*, Mon. Not. R. Astron. Soc. **328**, 1039 (2001).
[19] 2dFGRS Team, W.J. Percival *et al.*, Mon. Not. R. Astron. Soc. **327**, 1297 (2001).
[20] 2dFGRS Team, O. Lahav *et al.*, Mon. Not. R. Astron. Soc. **333**, 961 (2002).
[21] 2dFGRS Team, L. Verde *et al.*, Mon. Not. R. Astron. Soc. **335**, 432 (2002).
[22] SDSS Collaboration, M. Tegmark *et al.*, Astrophys. J. **606**, 702 (2004).
[23] SDSS Collaboration, M. Tegmark *et al.*, Phys. Rev. D **69**, 103501 (2004).
[24] S. Hannestad, J. Cosmol. Astropart. Phys. **05**, 004 (2003).
[25] V. Barger, D. Marfatia, and A. Tregre, hep-ph/0312065.
[26] S. Hannestad, Phys. Rev. Lett. **85**, 4203 (2000).
[27] S. Esposito, G. Mangano, A. Melchiorri, G. Miele, and O. Pisanti, Phys. Rev. D **63**, 043004 (2001).
[28] J.P. Kneller, R.J. Scherrer, G. Steigman, and T.P. Walker, Phys. Rev. D **64**, 123506 (2001).
[29] S. Hannestad, Phys. Rev. D **64**, 083002 (2001).
[30] S.H. Hansen, G. Mangano, A. Melchiorri, G. Miele, and O. Pisanti, Phys. Rev. D **65**, 023511 (2002).
[31] R. Bowen, S.H. Hansen, A. Melchiorri, J. Silk, and R. Trotta, Mon. Not. R. Astron. Soc. **334**, 760 (2002).
[32] P. Crotty, J. Lesgourgues, and S. Pastor, Phys. Rev. D **67**, 123005 (2003).
[33] E. Pierpaoli, Mon. Not. R. Astron. Soc. **342**, L63 (2003).
[34] S. Hannestad and G. Raffelt, J. Cosmol. Astropart. Phys. **04**, 008 (2004).
[35] P. Crotty, J. Lesgourgues, and S. Pastor, Phys. Rev. D **69**, 123007 (2004).
[36] U. Seljak and M. Zaldarriaga, Astrophys. J. **469**, 437 (1996).
[37] M. Tegmark, A.J. Hamilton, and Y. Xu, Mon. Not. R. Astron. Soc. **335**, 887 (2002).
[38] M. Kawasaki, K. Kohri, and T. Moroi, astro-ph/0402490.
[39] K. Hagiwara *et al.*, Phys. Rev. D **66**, 010001 (2002).
[40] G. G. Raffelt, *Stars As Laboratories For Fundamental Physics: The Astrophysics Of Neutrinos, Axions, And Other Weakly Interacting Particles* (University of Chicago Press, Chicago, 1996).
[41] V. Berezinsky and J.W.F. Valle, Phys. Lett. B **318**, 360 (1993).
[42] R. Tomas, H. Paes, and J.W.F. Valle, Phys. Rev. D **64**, 095005 (2001); M. Kachelriess, R. Tomas, and J.W.F. Valle, *ibid.* **62**, 023004 (2000).
[43] K. Benakli and S. Davidson, Phys. Rev. D **60**, 025004 (1999).
[44] S. Bashinsky and U. Seljak, Phys. Rev. D **69**, 083002 (2004).